Journal of Computer Science 5 (1): 71-78, 2009
ISSN 1549-3636

Error Free Iterative Morphological Decomposition Algorithm for Shape Representation

[1]V. Vijaya Kumar, [2]A. Srikrishna and [3]G. Hemantha Kumar
[1]Department of Computer Science and Engineering and Information Technology,
Godavari Institute of Engineering and Technology, Rajahmundry, India
[2]Department of Computer Science and Engineering, Rayapati Venkat Ranga Rao and Jagarlamudi,
Chandramouli College of Engineering Guntur, India
[3]Department of Studies in Computer Science, University of Mysore, Karnataka, India

Abstract: Problem statement: A generalized skeleton transform allows a shape to be represented as a collection of modestly overlapped octagonal shape parts. One problem with several generalized Morphological skeleton transforms is that they generate noise after decomposition. The noise rate may not be effective for ordinary images; however this effect will be more when applied on printed or handwritten characters. **Approach:** The present study tackled this issue by applying a noise removal algorithm after morphological decomposition. **Results:** The algorithm was applied on various types of decomposition images. The Present method was compared with generalized skeleton algorithm and octagon-generating decomposition algorithm. **Conclusion:** The error rates with original image were evaluated using various error functions. The experimental results indicated that the present decomposition algorithm produces images with good clarity when compared with other algorithms.

Key words: Shape, noise, printed hand written characters, error-rate, error functions

INTRODUCTION

SHAPE representation is an important issue in image processing and computer vision. Efficient shape representation provides the foundation for the development of efficient algorithms for many shape-related processing tasks, such as image coding[1,2], shape matching and object recognition[3-7], content-based video processing[8,9] and image data retrieval[10,11]. Mathematical morphology is a shape-based approach to image processing[12,13]. Basic morphological operations can be given interpretations using geometric terms of shape, size and distance. Therefore, mathematical morphology is especially suited for handling shape-related processing and operations. Mathematical morphology also has a well-developed mathematical structure, which facilitates the development and analysis of morphological image processing algorithms. A number of morphological shape representation schemes have been proposed[1,2,14-28,30]. Many of them use the structural approach. That is, a given shape is described in terms of its simpler shape components and the relationships among the components.

The notion of skeleton or medial axis transform was first introduced by Blum[34]. Lantuejoul showed that the skeleton can be computed using morphological operations[35]. The term 'Skeleton' is often used to describe thinning algorithms that preserve homotopy but do not necessarily support exact shape reconstruction[36,37]. In this study, our focus is on building efficient structural shape representations that allow exact as well as approximate reconstructions of the input shapes. Therefore, we are following a structural and algebraic approach to shape representation. Recently new algorithms for skeletonization and thinning, for 2D images based on primitive concept approach were proposed[31-33].

The 'Morphological Skeleton Transform' (MST) is a leading morphological shape representation algorithm[14]. In the MST, a given shape is represented as a union of all maximal disks contained in the shape. In general, there is much overlapping among the maximal disks. The 'Morphological Shape Decomposition' (MSD) is another important morphological shape representation scheme[15], in which a given shape is represented as a union of certain

Corresponding Author: V. Vijaya Kumar, Department of Computer Science and Engineering and Information Technology, Godavari Institute of Engineering and Technology, Rajahmundry, India

disks contained in the shape. The overlapping among representative disks of different sizes is eliminated. A new morphological shape representation algorithm that can be viewed as a compromise between the MST and the MSD was recently proposed[23,29]. In this scheme, overlapping among representative disks of different sizes is allowed, but severe overlapping among such disks is avoided. This algorithm is called as 'Overlapped Morphological Shape Decomposition' (OMSD). The advantages of these basic algorithms include that they have simple and well-defined mathematical characterizations and they are easy and efficient to implement. This study focuses on building efficient structural shape representations that allow exact as well as approximate reconstructions of the input shapes.

MATERIALS AND METHODS

In this study, we will first introduce an algorithm for generating skeleton points which will find a special maximal octagon for each image point of a given shape. In the decomposition algorithm a given shape will be decomposed into a collection of modestly overlapping disk components. And it will also provide enough information to allow efficient collection of disk components to be selected for exact representation of the given shape. The exact representation of the given shape is achieved through a noise removal algorithm.

An algorithm for representation of skeleton points of a given image in the form of flow chart is shown in Fig. 1. In this algorithm, the skeleton points are derived by repeatedly applying erosion operation using eight structuring elements in the following order: $B_0, B_1, ...B_7, B_0, B_1, ...B_7, B_0, B_1, ...$ as shown in Fig. 2 The symbols '*','_', '+' represents origin, zero and one respectively. That is these eight structuring elements will be applied in cyclic sequence. This process of representation of skeleton points is same as 'octagon-generating decomposition algorithm.

The proposed (EFMD) Error Free Morphological Decomposition algorithm, while reconstructing the image removes noise and this is given in the form of a flow chart in Fig. 3 The proposed algorithm utilizes the number of skeleton points, in their co-ordinate positions, corresponding structuring elements and noise removal filter for reconstruction of the image. The process will be repeated for the skeleton points obtained by the algorithm to generate skeleton points shown in Fig. 1.

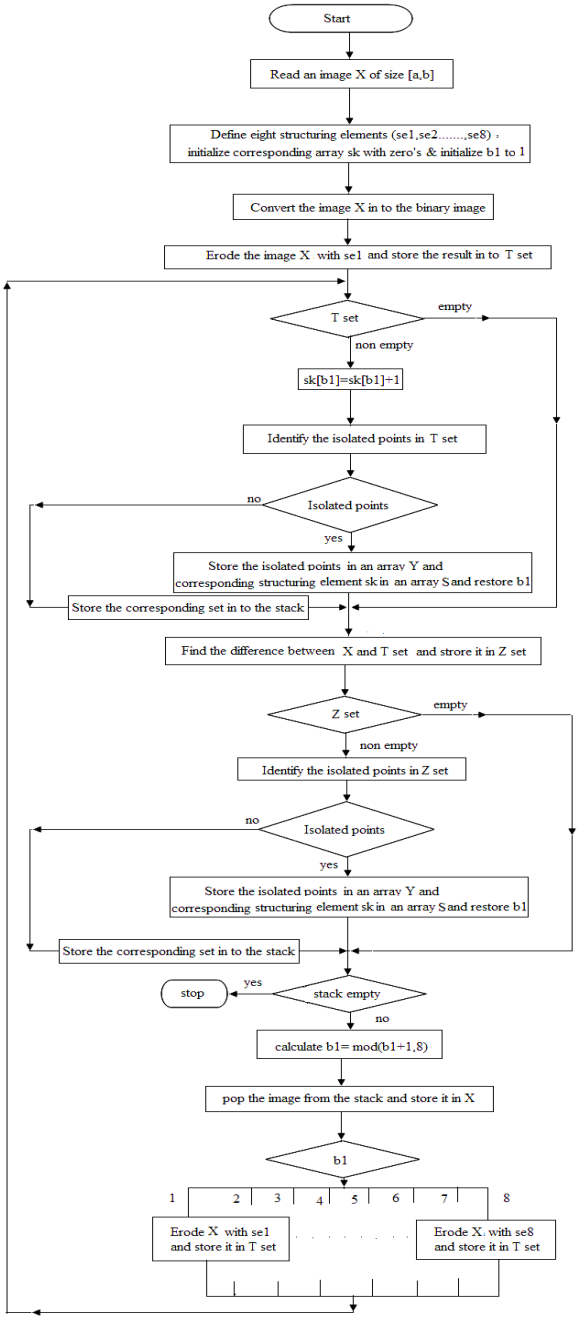

Fig. 1: Flowchart for algorithm to generate skeleton points

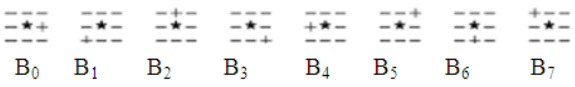

Fig. 2: Eight two-point structuring elements

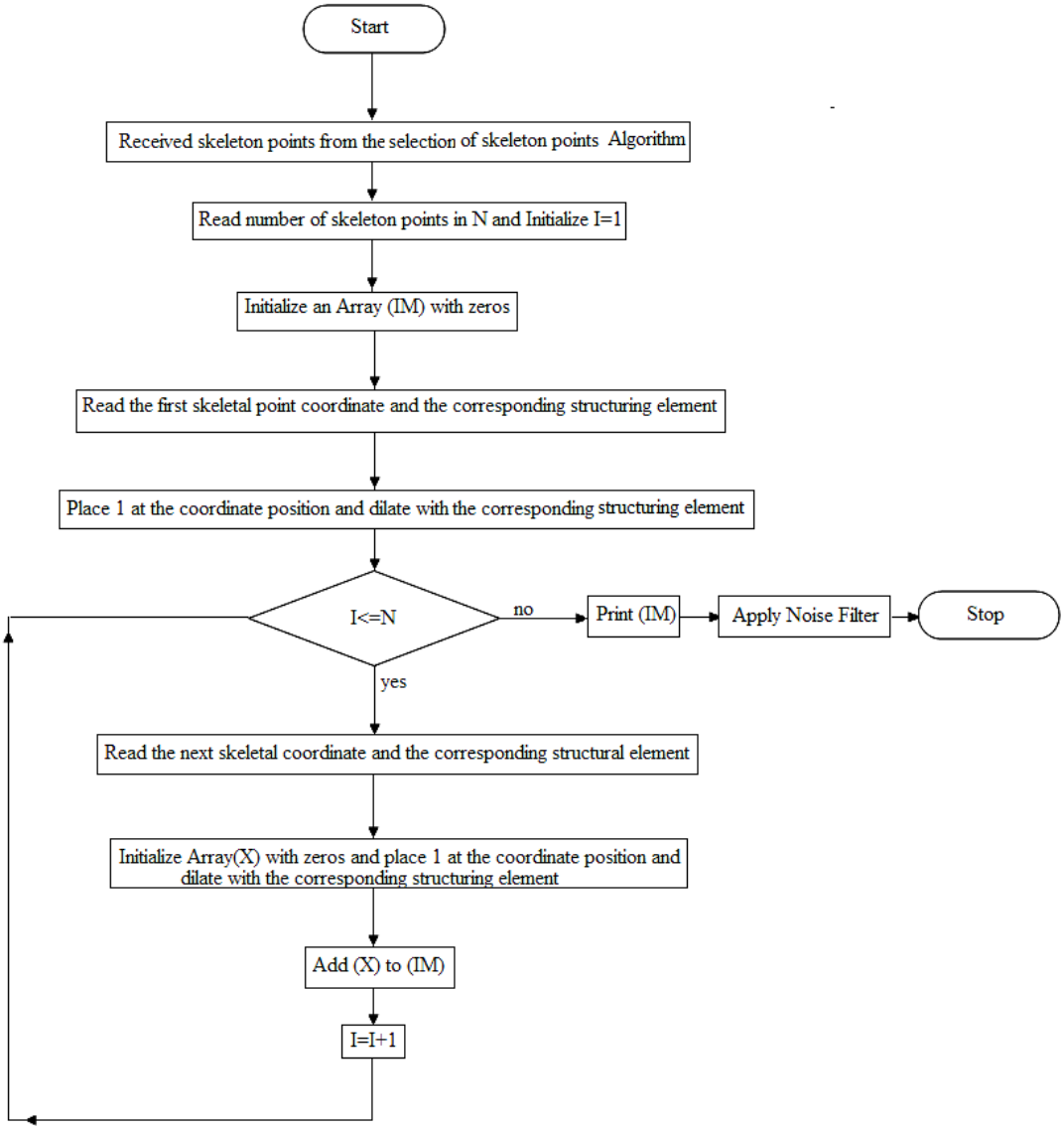

Fig. 3: Flowchart for noise removal for reconstruction of image

RESULTS

To test the integrity of the noise removal decomposition algorithm nine different images are taken and they are showed in the Fig. 4. Figure 5-7 show the reconstructed images using (GST) Generalized Skeleton Transform algorithm, (OGD) Octagon-Generating Decomposition algorithm and (EFMD) Error Free Morphological Decomposition algorithm. Various error functions as stated in equation (1-7) are applied on all reconstructed images using the three algorithms. The error rate is defined as the ratio between the number of image points that are not represented and the number of points in the original shape.

Error functions:

AEPP : Average error per pixel
MSE : Mean square error
RMSE : Root mean square error
SNR (ms) : Signal to noise ratio (mean square)
SNR (rms) : Signal to noise ratio (root mean square)
PSNR : Peak signal to noise ratio
Error-Rate : Error-rate per pixel

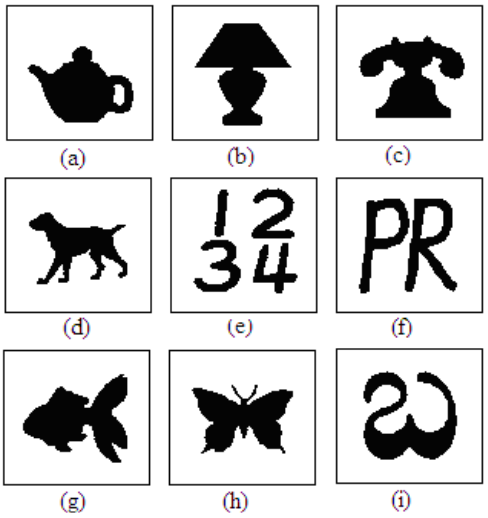

Fig. 4: Shape images used in the experiments. (a): Teapot; (b): Lamp; (c): Telephone; (d): Dog; (e): Digits; (f): Letters; (g): Fish; (h): Butterfly; (i): Telugu character

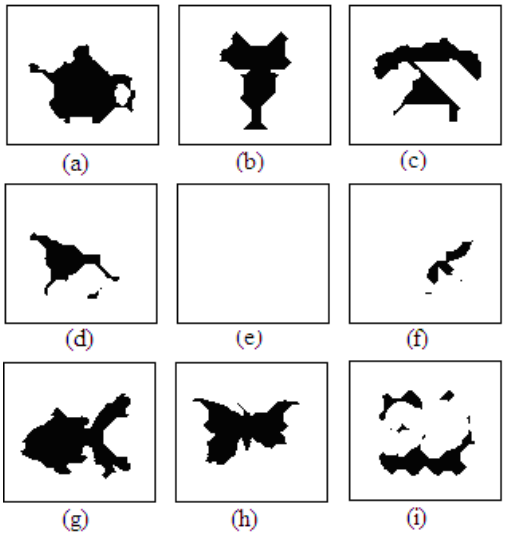

Fig. 5: Shape images after reconstruction using GST algorithm. (a): Teapot; (b): Lamp; (c): Telephone; (d): Dog (e): Digits; (f): Letters; (g): Fish; (h): Butterfly; (i): Telugu character

$$AEPP = \frac{1}{M \times N} \sum_{i=0}^{M-1} \sum_{j=0}^{N-1} \left| f(x,y) - g(x,y) \right| \quad (1)$$

$$MSE = \frac{1}{M \times N} \sum_{i=0}^{M-1} \sum_{j=0}^{N-1} (f(x,y) - g(x,y))^2 \quad (2)$$

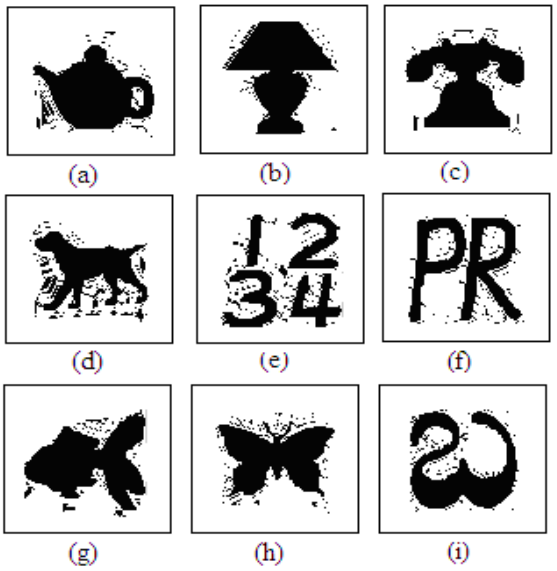

Fig. 6: Shape images after reconstruction using OGD algorithm. (a): Teapot; (b): Lamp; (c): Telephone; (d): Dog (e): Digits; (f): Letters; (g): Fish; (h): Butterfly; (i): Telugu character

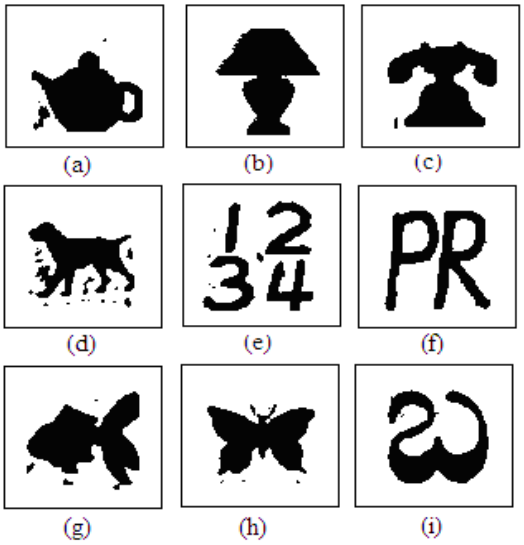

Fig. 7: Shape images after reconstruction using EFMD algorithm. (a): Teapot; (b): Lamp; (c): Telephone; (d): Dog; (e): Digits; (f): Letters; (g): Fish; (h): Butterfly; (i): Telugu character

$$RMSE = \sqrt{\frac{1}{M \times N} \sum_{i=0}^{M-1} \sum_{j=0}^{N-1} (f(x,y) - g(x,y))^2} \quad (3)$$

$$SNR(ms) = \frac{\sum_{i=0}^{M-1}\sum_{j=0}^{N-1} g(x,y)^2}{\sum_{i=0}^{M-1}\sum_{j=0}^{N-1} (g(x,y) - f(x,y))^2} \quad (4)$$

$$SNR(rms) = \sqrt{\frac{\sum_{i=0}^{M-1}\sum_{j=0}^{N-1} g(x,y)^2}{\sum_{i=0}^{M-1}\sum_{j=0}^{N-1} (g(x,y) - f(x,y))^2}} \quad (5)$$

$$PSNR = 10 * \log_{10}\left(\frac{255^2}{MSE}\right) \quad (6)$$

$$Error\_Rate = \frac{\sum_{i=0}^{M-1}\sum_{j=0}^{N-1} |f(x,y) - g(x,y)|}{\sum_{i=0}^{M-1}\sum_{j=0}^{N-1} f(x,y)} \quad (7)$$

Let:

$f(x,y)$ = Represent an input image

$g(x,y)$ = Represent reconstructed image

M and N = The sizes of input image and reconstructed image

A closely related objective measure is MSE. RMSE, SNR(ms), SNR(rms), PSNR are the defacto standards used in the image processing community. It is so commonly used for three reasons 1) because some objective measure is needed; (2) because it is possible to relate MSE to theoretical issues related to rate/distortion curves and least-squares minimization in statistical theory more easily than with any other measures and (3) because PSNR is a logarithmic measure which correlates with the logarithmic response to image intensity of the HVS. Generally speaking, as a rule of thumb, the higher PSNR will frequently correspond to better decompression noticeably. But the present study has tested this for reconstruction of the images.

DISCUSSION

All the error functions reflect this fact between the original image $f(x,y)$ and the reconstructed image $g(x,y)$. Table 1-3 show the error rates of reconstructed images with original image using GST algorithm, OGD algorithm and the EFMD algorithm, respectively. Table 1-3 average error rate of error functions on all nine different images is evaluated. It is evident that the error rate of the present method is reduced to half or even more when compared with other two algorithms.

One more interesting point is that the error rate of the proposed method is less than the other two methods for all images by using all error functions. The PSNR is high for the present method for all images. It indicates that it has high signal to noise ratio. Figure 8-10 show reconstructed images after reversing the background color of the image for generalized skeleton algorithm, octagon generating decomposition algorithm and, proposed error free decomposition algorithm respectively. Even in this case the proposed error free reconstruction algorithm has shown less noise when compared with other algorithms. The above fact is evident from the Table 4-6. When we reverse the background of the image, the shape component is not clear with GST, due to the effect of dilation on background intensity as shown in Fig. 5. By this, error rate is increased.

Fig. 8: Shape images after reconstruction using GST algorithm with image and background inverted. (a): Teapot; (b): Lamp; (c): Telephone; (d): Dog

Fig. 9: Shape images after reconstruction using OGD algorithm with image and background inverted: (a): Teapot; (b): Lamp; (c): Telephone; (d): Dog

Fig. 10: Shape images after reconstruction and using EFMD algorithm with image and background inverted (a): Teapot; (b): Lamp; (c): Telephone; (d): Dog

Table 1: Error calculations using different error functions after reconstruction using generalized skeleton transform algorithm

	AEPP	MSE	RMSE	SNR (ms)	SNR (rms)	PSNR	Error-rate
Teapot	0.061020000	0.061020000	0.24702000	11.04700	3.3237000	60.276000	9.953400
Lamp	0.180820000	0.180820000	0.42523000	4.130900	2.0325000	55.558000	31.93900
Telephone	0.170610000	0.170610000	0.41305000	4.367200	2.0898000	55.811000	29.69800
Dog	0.133270000	0.133270000	0.36506000	6.494600	2.5485000	56.884000	18.20000
Digits							
Letters	0.280820000	0.280820000	0.52992000	3.389500	1.8411000	53.647000	41.84900
Fish	0.071020000	0.071020000	0.26650000	9.069000	3.0115000	59.617000	12.39300
Butterfly	0.077755000	0.077755000	0.27885000	9.343800	3.0568000	59.224000	11.98500
Telugu character	0.197750000	0.197750000	0.44470000	3.950600	1.9876000	55.170000	33.89100
Average	0.146633125	0.146633125	0.37129125	6.474075	2.4864375	57.023375	23.73855

Table 2: Error calculations using different error functions after reconstruction using octagon-generating decomposition algorithm

	AEPP	MSE	RMSE	SNR (ms)	SNR (rms)	PSNR	Error-rate
Teapot	0.04286	0.04286	0.20702	13.32400	3.65020	61.81100	6.99070
Lamp	0.02633	0.02633	0.16225	20.50400	4.52810	63.92700	4.65030
Telephone	0.02980	0.02980	0.17261	18.28100	4.27560	63.38900	5.18650
Dog	0.08490	0.08490	0.29137	7.62500	2.76130	58.84200	11.59400
Digits	0.06347	0.06347	0.25193	9.93890	3.15260	60.10500	9.14170
Letters	0.04000	0.04000	0.20000	15.86700	3.98340	62.11000	5.96110
Fish	0.03755	0.03755	0.19378	14.26100	3.77640	62.38500	6.55270
Butterfly	0.03837	0.03837	0.19588	15.91000	3.98870	62.29100	5.91380
Telugu character	0.04028	0.04028	0.20071	13.48500	3.67220	62.08000	6.90380
Average	0.04484	0.04484	0.20839	14.35510	3.75428	61.88222	6.98829

Table 3: Error calculations using different error functions after reconstruction using error free decomposition algorithm

	AEPP	MSE	RMSE	SNR (ms)	SNR (rms)	PSNR	Error-rate
Teapot	0.02531	0.02531	0.15908	21.31500	4.61680	64.09900	4.12780
Lamp	0.01531	0.01531	0.12372	32.89300	5.73530	66.28200	2.70370
Telephone	0.01429	0.01429	0.11952	35.94300	5.99520	66.58200	2.48670
Dog	0.05000	0.05000	0.22361	12.66100	3.55830	61.14100	6.82830
Digits	0.02878	0.02878	0.16963	21.59600	4.64710	63.54100	4.14460
Letters	0.01857	0.01857	0.13628	32.62600	5.71200	65.44200	2.76760
Fish	0.02143	0.02143	0.14639	23.58100	4.85600	64.82100	3.73930
Butterfly	0.01653	0.01653	0.12857	35.50600	5.95870	65.94800	2.54800
Telugu character	0.02075	0.02075	0.14406	24.81200	4.98110	64.96000	3.55650
Average	0.02344	0.02344	0.15010	26.77033	5.11783	64.75733	3.65583

Table 4: Error calculations using different error functions after reconstruction using generalized skeleton transform algorithm (image and background inverted)

	AEPP	MSE	RMSE	SNR (ms)	SNR (rms)	PSNR	Error-Rate
Teapot	0.07000	0.07000	0.26458	6.52770	2.55490	59.68000	18.09100
Lamp	0.02000	0.02000	0.14142	22.69400	4.76380	65.12100	4.60960
Telephone	0.01122	0.01122	0.10595	38.90900	6.23770	67.62900	2.63790
Dog	0.03490	0.03490	0.18681	8.67250	2.94490	62.70300	13.03400
Average	0.03403	0.03403	0.17469	19.20080	4.12533	63.78325	9.59313

Table 5: Error calculations using different error functions after reconstruction using octagon-generating decomposition algorithm (image and background inverted)

	AEPP	MSE	RMSE	SNR (ms)	SNR (rms)	PSNR	Error-Rate
Teapot	0.01122	0.01122	0.10595	33.72700	5.80750	67.62900	2.90080
Lamp	0.07939	0.07939	0.28176	4.46530	2.11310	59.13300	18.29700
Telephone	0.02225	0.02225	0.14915	18.12800	4.25780	64.65800	5.22780
Dog	0.02449	0.02449	0.15649	9.93330	3.15170	64.24100	9.14630
Average	0.03434	0.03434	0.17334	16.56340	3.83253	63.91525	8.89298

Table 6: Error calculations using different error functions after reconstruction using error free decomposition algorithm.(image and background inverted)

	AEPP	MSE	RMSE	SNR (ms)	SNR (rms)	PSNR	Error-Rate
Teapot	0.00714	0.00714	0.08452	54.40000	7.37560	69.59200	1.84600
Lamp	0.06694	0.06694	0.25873	5.45730	2.33610	59.87400	15.42800
Telephone	0.00898	0.00898	0.09476	47.59100	6.89860	68.59800	2.11030
Dog	0.01714	0.01714	0.13093	15.10700	3.88680	65.79000	6.40240
Average	0.02505	0.02505	0.14223	30.63883	5.12428	65.96350	6.44668

CONCLUSION

In this study, we have introduced an error free decomposition algorithm. By this, noise rate is reduced. The proposed noiseless decomposition algorithm is more efficient than generalized skeleton algorithm or octagon-generating decomposition algorithm. The experimental results using seven error functions on nine images show that the new error free decomposition algorithm produces a more clarity-based shape representation than the other two algorithms.

ACKNOWLEDGEMENT

The researchers would like to express their gratitude to Sri K.V.V. Satya Narayana Raju, Chairman and K. Sashi Kiran Varma, Managing Director, Chaitanya group of Institutions for providing necessary infrastructure. And they would like to thank Dr.G.V.S.Ananta Lakshmi for her invaluable suggestions and constant encouragement that led to improvise the presentation quality of this study.

REFERENCES

1. Hasan, Y.M.Y. and L.J. Karam, 2000. Morphological reversible contour representation. IEEE Trans. Patt. Anal. Mach. Intell., 22: 227-240. http://www2.computer.org/portal/web/csdl/doi/10.1109/34.841755
2. Kresch, R. and D. Malah, 1998. Skeleton-based morphological coding of binary images. IEEE Trans. Image Process., 7: 1387-1399. ieeexplore.ieee.org/iel4/83/15529/00718480.pdf?arnumber=718480
3. Pitas, I. and A. Maglara, 1991. Range image analysis using morphological signal decomposition. Patt. Recog., 24: 165-181. DOI: 10.1016/0031-3203(91)90086-K
4. Trahanias, P.E., 1992. Binary shape recognition using the morphological skeleton transform. Patt. Recog., 25: 1277-1288. DOI: 10.1016/0031-3203(92)90141-5
5. Ei-Kwae, E.A. and M.R. Kabuka, 2000. Binary object representation and recognition using the Hilbert morphological skeleton transform. Patt. Recog., 33: 1621-1636. DOI: 10.1016/S0031-3203(99)00169-7
6. Belongie, S., J. Malik and J. Puzicha, 2002. Shape matching and object recognition using shape contexts. IEEE Trans. Patt. Anal. Mach. Intell., 24: 509-522. DOI: 10.1109/34.993558
7. Siddiqi, K., A. Shokoufandeh, S.J. Dickinson and S.W. Zucker, 1999.Shock graphs and shape matching. Int. J. Comput. Vis., 35: 13-32. DOI: 10.1023/A:1008102926703
8. Salembier, P., P. Brigger, J.R. Casas and M. Pardas, 1996. Morphological operators for image and video compression. IEEE Trans. Image Process., 5: 881-897. http://gps-tsc.upc.es/imatge/_Montse/publication_data.html
9. Jasinschi, R.S. and J.M.F. Moura, 1995. Content-based video sequence representation., Proceeding of the IEEE International Conference Image Processing, Oct. 23-26, IEEE Computer Society, Washington, DC., USA., pp: 2229. http://portal.acm.org/citation.cfm?id=841149&dl=GUIDE&coll=GUIDE&CFID=26503854&CFTOKEN=73362793
10. Sharvit, D., J. Chan, H. Tek and B. Kimia, 1998. Symmetry-based indexing of image databases. J. Vis. Commun. Image Represent., 9: 366-380. http://www.lems.brown.edu/~des/papers/symmetry_based_indexing-CVPR98.ps.gz
11. Latecki, L.J. and R. Lakamper, 2002. Application of planar shape comparison to object retrieval in image databases. Patt. Recog., 35: 15-29. DOI: 10.1016/S0031-3203(01)00039-5
12. Serra, J., 1983. Image Analysis and Mathematical Morphology. Academic, London, UK., ISBN: 10: 0126372403, pp: 610.
13. Haralick, R.M., S.R. Sternberg and X. Zhuang, 1987. Image analysis using mathematical morphology. IEEE Trans. Patt. Anal. Mach. Intell., 9: 532-550. http://portal.acm.org/citation.cfm?id=28802
14. Maragos, P.A. and R.W. Schafer, 1986. Morphological skeleton representation and coding of binary images. IEEE Trans. Acoust. Speech Signal Process., 34: 1228-1244. http://ieeexplore.ieee.org/xpl/freeabs_all.jsp?arnumber=1164959
15. Pitas, I. and A.N. Venetsanopoulos, 1990. Morphological shape decomposition. IEEE Trans. Pattern Anal. Mach. Intell., 12: 38-45. DOI: 10.1109/34.41382
16. Reinhardt, J.M. and W.E. Higgins, 1996. Comparison between the morphological skeleton and morphological shape decomposition. IEEE Trans. Patt. Anal. Mach. Intell., 18: 951-957. DOI: 10.1109/34.537351

17. Maragos, P., 1988. Morphology-based symbolic image modeling multi-scale nonlinear smoothing and pattern spectrum. Proceedings of the Conference on Computer Vision Pattern Recognition, June 5-9, IEEE Computer Society, Washington DC., USA., pp: 766-773. DOI: 10.1109/CVPR.1988.196321
18. Pitas, I. and A.N. Venetsanopoulos, 1992. Morphological shape representation. Patt. Recog., 25: 555-565. DOI: 10.1016/0031-3203(92)90073-R
19. Reinhardt, J.M. and W.E. Higgins, 1996. Efficient morphological shape representation. IEEE Trans. Image Process., 5: 89-101. http://ieeexplore.ieee.org/search/wrapper.jsp?arnumber=481673
20. Xu, J., 1996. Morphological decomposition of 2-D binary shapes into conditionally maximal convex polygons. Patt. Recog., 29: 1075-1104. http://ieeexplore.ieee.org/search/wrapper.jsp?arnumber=413538
21. Xu, J., 2001. Morphological representation of 2-D binary shapes using rectangular components. Patt. Recog., 34: 277-286. DOI: 10.1109/ICIP.1999.823020
22. Xu, J., 2001. Morphological decomposition of 2-D binary shapes into convex polygons: A heuristic algorithm. IEEE Trans. Image Process., 10: 61-71. DOI: 10.1109/83.892443
23. Xu, J., 2001. Efficient morphological shape representation with overlapping disk components. IEEE Trans. Image Process., 10: 1346-1356. DOI: 10.1109/83.941858
24. Xu, J., 2003. A generalized discrete morphological skeleton transform with multiple structuring elements for the extraction of structural shape components. IEEE Trans. Image Process., 12: 1677-1686. DOI: 10.1109/TIP.2003.819225
25. Xu, J., 2003. Efficient morphological shape representation by varying overlapping levels among representative disks. Patt. Recog., 36: 429-437. DOI: 10.1016/S0031-3203(02)00075-4
26. Held, A. and K. Abe, 1994. On the decomposition of binary shapes into meaningful parts. Patt. Recog., 27: 637-647. DOI: 10.1016/0031-3203(94)90043-4.
27. Ronse, C. and B. Macq, 1991. Morphological shape and region description. Signal Process., 25: 91-106. DOI: 10.1016/0165-1684(91)90041-G
28. Goutsias, J. and D. Schonfeld, 1991. Morphological representation of discrete and binary images. IEEE Trans. Signal Process., 39: 1369-1379. DOI: 10.1109/78.136543
29. Xu, J., 1998. Efficient morphological shape representation without searching. Proceedings of the IEEE International Conference on Image Processing, Oct. 4-7, IEEE Computer Society, Washington DC., USA., pp: 262-266. DOI: 10.1109/ICIP.1998.723360
30. Xu, J., 2007. Morphological decomposition of 2-D binary shapes into modestly overlapped octagonal and disk components. IEEE Trans. Image Process., 16: 337-348. DOI: 10.1109/TIP.2006.888328
31. Vijaya, V. and Kumar *et al*., 2008. An improved iterative morphological decomposition approach for image skeletonization. GVIP. J., 8: 47-54. www.icgst.com/gvip/Volume8/Issue1/P1150812004.pdf
32. Vijaya, V. and Kumar *et al.*, 2008. A new skeletonization method based on connected component approach. Int. J. Comput. Sci. Network Sec., 8: 133-137. paper.ijcsns.org/07_book/200802/20080218.pdf
33. Vijaya Kumar, V. *et al.*, 2006. A comparison on morphological skeleton transform with multiple structuring elements.pg.no-8. Proceedings of the International Conference on ICORG, June 6-8, NIRD Campus, Hyderabad. www.icorg.org/html/ICORG-Technical- program.pdf
34. Blum, H., 1967. A Transformation for Extracting New Descriptors of Shape. In: Models for the Perception of Speech and Visual Forms, Wathen-Dunn, W. (Ed.). MIT Press, Cambridge, MA., pp: 362-380.
35. Lantuejoul, C., 1980. Skeletonization in Quantitative Metallography. In: Issues of Digital Image Processing, Haralick, R.M. and J.C. Simon (Eds.). Sijthoff and Noordhoff, Groningen, Netherlands. DOI: 10.110910.1109/34.56190
36. Pudney, C., 1998. Distance-ordered homotopic thinning: A skeletonization algorithm for 3D digital images. Comput. Vis. Image Understand, 72: 404-413. DOI: 10.1006/cviu.1998.0680
37. Ranwez, V. and P. Soille, 2002. Order independent homotopic thinning for binary and grey tone anchored skeletons. Patt. Recog. Lett., 23: 687-702. DOI: 10.1016/S0167-8655(01)00146-5